

2023-05-29:

A revised version of this manuscript is now published at: <https://doi.org/10.1002/rse2.342>

## **TITLE**

Use of Airborne Laser Scanning to assess effects of understorey vegetation structure on nest-site selection and breeding performance in an Australian passerine bird

## **AUTHORS**

Richard S. Turner <sup>1,2 \*</sup>, Ophélie J. D. Lasne <sup>1</sup>, Kara N. Youngentob <sup>1,3</sup>, Shukhrat Shokirov <sup>1,3</sup>, Helen L. Osmond <sup>1</sup>, & Loeske E. B. Kruuk <sup>1,2</sup>

## **AFFILIATIONS**

<sup>1</sup> Division of Ecology & Evolution, Research School of Biology, Australian National University, Canberra, ACT 2601, Australia

<sup>2</sup> Institute of Ecology and Evolution, School of Biological Sciences, University of Edinburgh, Edinburgh EH9 3FL, United Kingdom

<sup>3</sup> The Fenner School of Environment & Society, Australian National University, Canberra, ACT 2601, Australia

\* Corresponding author. Email: [richard.turner@anu.edu.au](mailto:richard.turner@anu.edu.au)

## 1 **ABSTRACT**

2 In wild bird populations, the structure of vegetation around nest-sites can influence the risk of predation  
3 of dependent offspring, generating selection for nest-sites with vegetation characteristics associated  
4 with lower predation rates. However, vegetation structure can be difficult to quantify objectively in the  
5 field, which might explain why there remains a general lack of understanding of which characteristics  
6 are most important in determining predation rates. Airborne Laser Scanning (ALS) offers a powerful  
7 means of measuring vegetation structure at unprecedented resolution. Here, we combined ALS with 11  
8 years of breeding data from a wild population of superb fairy-wrens *Malurus cyaneus* in southeastern  
9 Australia, a species which nests relatively close to the ground and has high rates of nest and fledgling  
10 predation. We derived structural measurements of understorey (0-8 m) vegetation from a contiguous  
11 grid of 30 x 30 m resolution cells across our c. 65 hectare study area. We found that cells with nests  
12 (nest-cells) differed in their understorey vegetation structure characteristics compared to unused cells,  
13 primarily in having denser vegetation in the lowest layer of the understorey (0-2 m; the 'groundstorey'  
14 layer). The average height of understorey vegetation was also lower in cells with nests than in those  
15 without nests. However, relationships between understorey vegetation structure characteristics and  
16 breeding performance were mixed. Nest success rates decreased with higher volumes of groundstorey  
17 vegetation, as did fledgling survival rates, though only in nest-cells with lower height vegetation. Our  
18 results indicate that ALS can identify vegetation characteristics relevant for superb fairy-wren nest-site  
19 selection, but that nesting preferences are not beneficial under current predation pressures. The study  
20 illustrates the potential for using ALS to investigate how ecological conditions affect behaviour and life-  
21 histories in wild animal populations.

22

23 Keywords: "Airborne Laser Scanning", "LiDAR", "Vegetation Structure", "Avian Breeding  
24 Performance", "Nest Predation", "Nest-Site Selection"

25

## 26 **INTRODUCTION**

27 Dependent offspring of many wild animal populations are frequently vulnerable to predation. The  
28 importance of dependent offspring predation for the evolution and plasticity of adult breeding  
29 behaviours is increasingly recognised in evolutionary and behavioural ecology (Ibáñez-Álamo et al.,  
30 2015; Lima, 2009; Lima & Dill, 1990). Studies of birds provide an excellent system to explore the  
31 determinants and consequences of dependent offspring predation. The loss to predation of eggs and

32 nestlings in nests (nest predation) is often the primary determinant of avian breeding failure (Martin,  
33 1993; Ricklefs, 1969), and globally, rates of nest predation may have increased in recent decades  
34 (Kubelka et al., 2018; Matysioková & Remeš, 2022; Remeš et al., 2012a, 2012b). Even after leaving the  
35 nest, fledglings can suffer high mortality, mostly due to predation (Naef-Daenzer & Gruebler, 2016;  
36 Naef-Daenzer et al., 2001). Understanding nest and fledgling predation is therefore central to  
37 understanding the ecological pressures that shape bird breeding behaviours and life-histories, and for  
38 informing conservation and management strategies for imperilled species.

39

40 The density and complexity of vegetation surrounding a nest can determine the predation of both the  
41 nest and fledglings. Denser and more complex vegetation is thought to reduce visual and auditory cues  
42 to predators, and to create a physical barrier that impedes predators or reduces their searching  
43 efficiency (Bowman & Harris, 1980; Filliater et al., 1994; Magrath et al., 2010; Martin, 1993; Martin &  
44 Roper, 1988; Mouton & Martin, 2019). However, although natural selection should therefore favour  
45 sites with denser and more complex vegetation, especially when primary predators are visually or  
46 auditorily-oriented, there is limited evidence to date that nest-sites with such structural vegetation  
47 characteristics have reduced predation rates (Borgmann & Conway, 2015; Lahti, 2009). This may be  
48 because predators are not hindered in the way we expect. However, another possibility is that previous  
49 studies have not been able to measure vegetation structure characteristics with sufficient resolution. In  
50 part due to the high cost and labour intensive nature of manually collecting accurate and precise data,  
51 previous studies have often relied on structural vegetation data that were visually-estimated and taken  
52 from a subset of available locations, but evidence suggests that such data may be researcher-biased and  
53 not representative of the broader landscape (Block et al., 1987; Gotfryd & Hansell, 1985).

54

55 Active remote sensing such as Light Detection and Ranging (LiDAR) can provide an effective method  
56 for accurately and reliably assessing vegetation structure due to its ability to provide high-resolution  
57 and spatially contiguous data in a standardised and comparable way (Lefsky et al., 2002; Moudrý et al.,  
58 2023; Vierling et al., 2008). Airborne Laser Scanning (ALS) (i.e., a LiDAR sensor mounted on an  
59 aircraft) is the most common method for collecting LiDAR data and uses laser pulses to measure the  
60 coordinates ( $x, y, z$ ) of reflective surface objects (Wehr & Lohr, 1999). As the timing and position of the  
61 sensor on the aircraft are known, the distance to each object can be calculated precisely and a three-  
62 dimensional “point cloud” can be derived (Lefsky et al., 2002; Vierling et al., 2008). Additional

63 attributes can be specified for each point during processing that can be used to calculate structural  
64 vegetation characteristics (Bakx et al., 2019; Davies & Asner, 2014). While some studies have used ALS  
65 data to investigate questions in evolutionary and behavioural ecology, they have generally focused on  
66 species abundance, richness, and distribution modelling in relation to vegetation structure (Ciuti et al.,  
67 2017; Davies & Asner, 2014; de Vries et al., 2021; Moudrý et al., 2023; Shokirov et al., 2023). However,  
68 with the increasing availability of ALS data (Moudrý et al., 2023), recent research has shown the  
69 potential of combining such data with detailed behavioural and life-history data of single animal  
70 populations (Davies et al., 2016, 2019; Hill & Hinsley, 2015; Hill et al., 2004; Klein et al., 2020). For  
71 example, Klein et al. (2020) used ALS data spanning 8300 hectares in an analysis of the breeding  
72 success of Siberian jays *Perisoreus infaustus* and found a positive association between increased  
73 understorey vegetation density and breeding success for birds in territories close to human settlements,  
74 which are an indicator of the occurrence of their main nest predator, the Eurasian jay *Garrulus*  
75 *glandarius*. The broad spatial coverage of the ALS data used in their study enabled the identification of  
76 relationships that would have been difficult to discover using traditional methods.

77

78 In this study, we used 11 years of detailed, individual-based breeding data to investigate the associations  
79 between vegetation structure and nest and fledgling predation in a population of superb fairy-wrens  
80 *Malurus cyaneus* in southeastern Australia. Although superb fairy-wrens mostly forage in open grassy  
81 areas (Schlotfeldt & Kleindorfer, 2006), they build their nests close to the ground in dense vegetation,  
82 such as grass tussocks or small shrubs, which are subject to high levels of nest and fledgling predation  
83 (Cockburn et al., 2016; Colombelli-Négrel & Kleindorfer, 2009; Rowley & Russell, 1997). Superb fairy-  
84 wrens have many nest and fledgling predators (Rowley & Russell, 1997), with their dominant predator  
85 being the pied currawong *Strepera graculina* in areas where the two species' ranges overlap  
86 (Prawiradilaga, 1996; Yasukawa & Cockburn, 2009). Indeed, pied currawongs have been implicated as  
87 an important predator of most small passerines throughout eastern and southeastern Australia (Bayly  
88 & Blumstein, 2001; Fulton & Ford, 2001; Fulton, 2019).

89

90 Pied currawongs are large, corvid-like, passerine birds that use visual and auditory cues to detect prey  
91 (Wood, 2000; Yasukawa & Cockburn, 2009). Given this searching method, we hypothesise, firstly, that  
92 superb fairy-wrens should favour nest-sites with denser and more complex vegetation, and secondly,  
93 that such nest-sites would experience lower rates of nest and fledgling predation. The first hypothesis

94 has not previously been tested for superb fairy-wrens. Contrary to the expectations of the second  
95 hypothesis, two previous studies of superb fairy-wrens have shown that increased vegetation density is  
96 associated with higher rates of nest predation and lower numbers of fledglings, when vegetation was  
97 measured in the immediate vicinity of the nest (Colombelli-Négrel & Kleindorfer, 2009) and at the  
98 broader territory-level (Backhouse et al., 2023), with the latter study conducted on the same population  
99 as this study. It is worth noting, however, that both these studies used visually-estimated measures of  
100 vegetation collected from a subset of locations, which were then summarised into relatively coarse  
101 metrics. Moreover, neither study examined whether the same characteristics were important for nest-  
102 site selection by comparing nest-sites with non-nesting sites.

103

104 The aim of this study was to test these two hypotheses regarding superb fairy-wrens and their breeding  
105 behaviour, using structural vegetation data derived from ALS. Because superb fairy-wrens nest close to  
106 the ground, we expected that the structure of the understorey vegetation, which we define here as 0 – 8  
107 m above ground, would be most important in determining nest-site selection and breeding performance  
108 in this species (Cockburn et al., 2016; Rowley & Russell, 1997). We therefore focused on three  
109 characteristics related to understorey vegetation height, complexity, and density, using a contiguous  
110 grid of 30 x 30 m resolution cells spanning our study area. We tested: (i) whether these understorey  
111 vegetation characteristics influenced nest-site selection; and (ii) whether nest-site selection was  
112 adaptive to in relation to predation pressures, by assessing associations of understorey vegetation  
113 characteristics with rates of nest success and fledgling survival.

114

## 115 MATERIALS AND METHODS

### 116 Study area

117 Our study area is located in Canberra, Australian Capital Territory, Australia (Figure 1) and  
118 encompasses an area of c. 65 hectares that includes a *managed* area in the Australian National Botanic  
119 Gardens (ANBG; c. 43 hectares) and an *unmanaged* area in the adjacent Black Mountain Nature  
120 Reserve (c. 22 hectares). The study area consists of broadly of mature open sclerophyll forest, with  
121 evergreen *Eucalyptus macrorhyncha* and *Eucalyptus rossii* as the primary tree species, and *Acacia*  
122 spp., *Callistemon* spp., *Notodanthonia* spp., *Rytidosperma palladium*, *Triodia scariosa*, and  
123 *Lomandra longifolia* as the dominant understorey shrubs and grasses. The *managed* area also includes  
124 a diverse collection of native vegetation established in dense plantings, and three semi-artificial habitats

125 (specifically, a ‘rainforest’ area, a ‘desert’ area, and a grass lawn). Along the eastern perimeter of the  
126 *unmanaged* area, there is a small patch of gullies that flood with rainwater that is dominated by  
127 *Bursaria spinosa*, and non-native species including *Rubus fruticosus* (Fraser & Purdie, 2020).

128

### 129 **Superb fairy-wren study population and data collection**

130 Superb fairy-wrens are facultative cooperative-breeders that live on year-round territories in groups  
131 composed of a dominant breeding pair and up to five male helpers (Cockburn et al., 2016; Rowley &  
132 Russell, 1997). Females are solely responsible for nest-building and incubation, but all group members  
133 defend and provision the brood. They have a long breeding season that runs between September and  
134 March (Lv et al., 2019). Hereafter, we refer to a given breeding season by the calendar year in which it  
135 commenced. The species is multi-brooded: high rates of nest predation mean a female superb fairy-  
136 wren may initiate as many as nine or ten clutches per breeding season, but often only one brood (if any)  
137 successfully reaches independence. Clutch sizes can range from one to five eggs but clutches with three  
138 eggs are most common (Cockburn et al., 2016; Rowley & Russell, 1997). Further details regarding the  
139 breeding behaviour of superb fairy-wrens in our study area are provided as Figure S1 – S4.

140

141 Two hailstorms damaged the study area on 27 February 2007 and 19 January 2020 respectively. In this  
142 study, we therefore constrained our analyses to data from 11 breeding seasons (from 2009 –2019; up  
143 until the hailstorm on 19 January 2020); this interval is centred around 2015 when the ALS data were  
144 collected (details below). The weather conditions were consistent during this time (Figure S5) and the  
145 structure of the vegetation remained unchanged. Thus, we did not expect any time difference between  
146 the superb fairy-wren breeding data in a given year and the ALS data to affect our ability to detect any  
147 relationships (Hill & Hinsley, 2015; Vierling et al., 2014). For completeness, we also repeated all  
148 analyses using data from 1994 – 2019 (the full duration during which breeding data have been collected  
149 across the full extent of our study area). We present these results separately as Table S1.

150

151 Between 2009 – 2019, the study area supported 34 – 79 superb fairy-wren territories each year, with  
152 an average territory size of  $1.09 \pm 0.71$  hectares (mean  $\pm$  SD,  $n = 686$  territory-years). Unique colour-  
153 banding of individuals in the study population allowed for individual recognition. To locate nests, we  
154 observed the dominant female on each territory during nest-building or incubation. The location of each  
155 nest was initially recorded using a Garmin eTrex Global Positioning System (GPS) (Garmin Co., Olathe,

156 Kansas, USA) or a GPS application on a mobile phone (Handy GPS, BinaryEarth, Australia), within a  
157 reported accuracy of  $\pm 5$  m for all devices. We then used a 30 m grid map of the study area to confirm  
158 nest locations to one decimal point fraction (i.e., within a 9 m<sup>2</sup> grid cell) based on recognisable physical  
159 landmarks in the study area (e.g., paths, buildings, and specific landscaping features). Thus, final nest  
160 locations were accurate to  $\pm 3$  m. Coordinates were collected in spatial reference Geocentric Datum of  
161 Australia 1994, Map Grid of Australia Zone 55 (Collier & Steed, 2001). All analyses presented here were  
162 subsequently conducted using this projection. We monitored the progress of each nest every second day  
163 for the duration of the nesting period (c. 24 days from the onset of incubation) to determine *nest fate*.  
164 Nests that fledged at least one offspring were considered *successful*. Nest predation was assumed when  
165 all eggs or nestlings disappeared prior to their expected fledging date. Because our interest was in  
166 whether nest-site selection influenced breeding performance via predation risk, we excluded 172 nests  
167 (9.35% of the total) that failed due to reasons other than predation (Figure S3). When nests were  
168 successful, we closely monitored individual fledglings to determine their survival to independence,  
169 defined as four weeks (28 days) post-fledging. Although most offspring were still being provisioned at  
170 this age, five-weeks post-fledging is the earliest known age of dispersal in our study area; this cut-off  
171 point therefore avoids any chance of dispersal being confused with mortality (Hajduk et al., 2018,  
172 2020). Causes of fledgling mortality were generally unknown, but the recovery of colour-bands of  
173 fledglings from pellets of pied currawongs suggests that predation is an important source of mortality  
174 (Prawiradilaga, 1996). In this study, we used all fledgling mortality as a measure of fledgling predation.  
175

176 Using the grid map of our study area as reference, we derived measurements of understorey vegetation  
177 structure at a 30 x 30 m resolution spanning the extent of our study area (n = 768 cells; further details  
178 are provided below; see also Backhouse et al., 2023). Because superb fairy-wren territories were on  
179 average 1.09 hectares in size, each 30 x 30 m resolution cell therefore encompassed c. 10% of the average  
180 territory. Each nest was then assigned to a cell based on its location. We excluded breeding data from  
181 25 cells (3.3% of the total) that encompassed the three semi-artificial habitats in the study area  
182 (described above), as superb fairy-wrens do not inhabit these regions of our study area because they  
183 contain vegetation that is very different from their native range. Breeding data from a further two cells  
184 were later excluded as they contained no understorey vegetation structure data (details below).

185

186 The superb fairy-wren breeding dataset used in this study therefore comprised of observations from a  
187 total of 1431 nests (from 318 females), encompassing 741 cells over 11 years ( $n = 8151$  cell-years). For  
188 analysis of nest-site selection, cell-years were subsequently designated as nest-cell-years (cell-years  
189 with a nest,  $n = 1094$  cell-years) or unused-cell-years (cell-years without a nest, 7057 cell-years). For  
190 each nest-cell-year we estimated two measures of breeding performance: (i) *nest success rate* and (ii)  
191 *fledgling survival rate*, both of which are defined in Table 1. In rare cases, more than one female  
192 occupied a given nest-cell-year – for example, in cases where cells overlapped territory boundaries, or  
193 the death of a female resulted in her being replaced by a different female. In these cases, observations  
194 were treated as independent for each female (female-nest-cell-year).

195

196 The number of nest-cells declined significantly over the course of the study (Figure S6a), a finding that  
197 is consistent with the observation of a 72.16% population decline of females during the period  
198 considered here (Figure S6b), and with a general decline across the entire study period (Backhouse et  
199 al., 2023; Lv et al., 2023). This decline in population size may be linked to increased rates of adult winter  
200 mortality associated with climate change (Lv et al., 2023). For the purpose of this study, and because  
201 we are focusing on a shorter time-scale, we do not consider this decline in detail.

202

### 203 **Airborne Laser Scanning data**

204 ALS data were collected between 21 May 2015 and 5 April 2016 by the Australian Capital Territory  
205 Government's Environment, Planning and Sustainable Development Directorate  
206 ([www.planning.act.gov.au](http://www.planning.act.gov.au)), using an AX60 scanner mounted to an aircraft (with a Riegl LMS-Q780  
207 sensor and Trimble AP50 GPS). Details of the ALS survey were as follows: flight elevation above ground  
208 level: 450 m; point density: 8 pulses/m<sup>2</sup>; footprint size: 0.12 m; swath width: 539 m; overlap: 25%;  
209 vertical precision:  $\pm 0.30$  m; horizontal precision:  $\pm 0.80$  m. Further details including the flight speed,  
210 laser wavelength, scan frequency, and pulse frequency were not provided with the dataset  
211 ([www.planning.act.gov.au](http://www.planning.act.gov.au)). The data were pre-processed by the vendor and came with a classification  
212 of *ground*, *building*, *water*, *vegetation*, and *noise* points, and were distributed in LAS v.1.4 format  
213 projected in spatial reference Geocentric Datum of Australia 1994, Map Grid of Australia Zone 55  
214 (Collier & Steed, 2001).

215



216 We separated the ALS data into each of our 30 x 30 m resolution cells using LAStools (rapidlasso GmbH;  
217 van Rees, 2013). Using the package 'lidR' (v.3.1.3; Roussel et al., 2020) in R (v.4.0.5; R Core Team,  
218 2021), we further processed the data to derive vegetation structure characteristics for each cell as  
219 follows: First, point cloud data were normalised by subtracting the height of ground points from the  
220 height of non-ground points (following e.g., Ciuti et al., 2017; Koma et al., 2021; Shokirov, 2021;  
221 Shokirov et al., 2023). Second, points classified as *ground*, *building*, *water*, and *noise* were removed,  
222 resulting in only points classified as *vegetation* being retained. A total of two cells were found to contain  
223 no *vegetation* points, and so were excluded from further processing. Third, *vegetation* points were  
224 categorised into two layers: *understorey layer* (0 – 8 m), and *canopy layer* (> 8 m). We used 8 m as  
225 the threshold distinguishing these two vegetation layers based on the distribution of the normalised z  
226 coordinates (height values) of the point cloud (Figure S7) and knowledge of the primary *Eucalyptus*  
227 spp. in the study area (Fraser & Purdie, 2020). We then removed *canopy vegetation* points from the  
228 point cloud data as we expected the structure of the understorey vegetation to be most relevant for  
229 superb fairy-wrens based on their nesting behaviour (Figure S1 – S2). Fourth, from the *understorey*  
230 *vegetation* points, we calculated the following three vegetation structure characteristics: (i) *mean*  
231 *height* of the understorey vegetation, (ii) *variation in height* of the understorey vegetation (as measured  
232 by the standard deviation, SD) and (iii) *volume* of the understorey vegetation. We initially calculated  
233 *volume* within four specific height thresholds (0 – 2 m, 2 – 4 m, 4 – 6 m, 6 – 8 m) but because the nests  
234 of superb fairy-wrens are generally <2 m above the ground, in our analyses we considered *volume* at  
235 the lowest height threshold only (hereafter referred to as '*groundstorey volume*'). Definitions of each of  
236 the three understorey vegetation structure characteristics are provided in Table 2. The final ALS point  
237 cloud dataset used in this study comprised a total of 1,686,744 understorey vegetation points, with a  
238 mean  $\pm$  SD of  $2270.18 \pm 1994.04$  points/cell.

239

## 240 **Statistical analysis**

241 Analyses were conducted using a Bayesian framework implemented in the package 'brms' (v.2.15.0;  
242 Bürkner, 2017) in R (v.4.0.5; R Core Team, 2021). Prior to analysis, explanatory parameters were mean  
243 standardised to allow for effect size comparisons (Harrison et al., 2018; Schielzeth, 2010), and potential  
244 multicollinearity (Dormann et al., 2013, Zuur et al., 2009) and spatial autocorrelation (Ciuti et al., 2017;  
245 Dormann et al., 2007) were assessed. Potential spatial autocorrelation was accounted for by including

246 a spatial conditional autoregressive (CAR) structure in our models (Bürkner, 2017; Dormann et al.,  
247 2007). Further details are provided as Appendix S1, Figure S8 – S9, and Table S2 – S3.

248

249 We constructed Bayesian spatial hierarchical generalised linear regression models for each of our three  
250 response variables of nest presence, nest success rate, and fledgling survival rate (Table 2). Each model  
251 included fixed effects of year (as a continuous covariate) plus the three understorey vegetation structure  
252 parameters. To account for repeated measurements of non-independent data, we included cell ID and  
253 year (as multi-level factors) as random effects. Female ID was additionally included as a random effect  
254 in the two models of breeding performance to account for multiple observations of the same female.

255

256 We initially also considered: non-linear effects of all understorey vegetation structure parameters; the  
257 two regions of the study area (as a two-level factor: managed, unmanaged); and two-way interactions  
258 between all explanatory parameters. Where these effects were non-significant, we discarded them from  
259 our final models (and do not present them here). Previous studies of superb fairy-wrens have shown  
260 positive associations between a female's age, the number of helpers, and different breeding performance  
261 metrics (e.g., Cockburn *et al.*, 2008; Hajduk *et al.*, 2020, 2021). We therefore included as fixed effects  
262 female age (as a two-level factor: 1 year old, 2+ year old, following e.g., Kruuk *et al.*, 2015; Hajduk *et al.*,  
263 2018) and number of helpers (as a two-level factor: 0 helpers, 1+ helpers, following e.g., Cooper *et al.*,  
264 2020; Taylor & Langmore, 2020) in our two models of breeding performance to control for their effects,  
265 but we do not focus on these effects in detail.

266

267 We ran all models on 4 independent MCMC chains for 8000 iterations, with a thinning interval of 10  
268 and a warm-up period of 3000 iterations (resulting in 2000 posterior samples), specifying weakly  
269 informative priors with a normal error distribution ( $\mu$ : 0;  $\sigma^2$ : 1; Gelman *et al.*, 2015). Effective sample  
270 sizes for specific parameters varied owing to autocorrelation, but they were always above 400 (a  
271 minimum effective sample size of 100 per chain; Vehtari *et al.*, 2021). Model convergence was confirmed  
272 by ensuring that potential scale reduction factors were  $< 1.01$  (Gelman *et al.*, 2013; Vehtari *et al.*, 2021).  
273 For each model, we assessed the goodness-of-fit using the posterior predictive check, *pp\_check*,  
274 function in the package 'bayesplot' (v.1.8.1; Gabry & Mahr, 2021). Unless stated otherwise, summary  
275 statistics are presented as means ( $\pm$  SE). Model parameter estimates are presented as posterior means

276 ( $\pm$  SD) and 95% credible intervals. We considered there to be statistical support for specific parameters  
277 when the 95% credible intervals do not span zero.

278

## 279 **RESULTS**

### 280 *Understorey vegetation structure parameters*

281 The mean ( $\pm$  SD) of the three understorey vegetation structure parameters were as follows: mean  
282 height:  $3.3 \pm 1.0$  m (Figure 2c); SD height:  $2.2 \pm 0.4$  m (Figure 2d); groundstorey volume:  $378.4 \pm 267.8$   
283  $\text{m}^3$  (Figure 2e). There was a positive correlation between mean height and SD height (Pearson  
284 correlation coefficient = 0.30), and negative correlations between mean height and groundstorey  
285 volume (Pearson correlation coefficient = -0.42) and between SD height and groundstorey volume  
286 (Pearson correlation coefficient = -0.25; Table S3).

287

### 288 *Nest-site selection*

289 Of the 741 cells, 39.41% ( $n = 292$  cells) never had a nest during the 11 years of our study, while 23.35%  
290 ( $n = 173$  cells) had a nest in only one year (Figure 1, Figure S10). The maximum number of years a cell  
291 had a nest was nine (two cells; Figure 1).

292

293 Nest presence in a cell decreased with increasing mean height (nest-cell-years:  $3.01 \pm 0.03$  m; unused-  
294 cell-years:  $3.33 \pm 0.01$  m; Table 3, Figure 3a – b), and increased with increasing groundstorey volume  
295 (nest-cell-years:  $477.20 \pm 8.53$   $\text{m}^3$ ; unused-cell-years:  $363.09 \pm 3.12$   $\text{m}^3$ ; Table 3, Figure 3c – d). Note,  
296 because a cell encompassed c. 10% of the average superb fairy-wren territory, random nest-site selection  
297 within a territory would mean an average probability of 0.10 of nest presence. Therefore, rates of nest  
298 presence  $>0.10$  indicate non-random site selection for particular cells (Figure 3b, d). We found no  
299 significant effect of SD height on nest presence (Table 3). However, this was possibly due to a lack of  
300 power in the 11 year subset of data (2009 – 2019) used in this analysis. Our analysis of the full dataset  
301 (1994 – 2019) did find statistical support for the positive association between SD height and nest  
302 presence, due to relatively smaller error around the parameter estimate (Table S1).

303

### 304 *Nest success rate*

305 Nest success rate was on average  $0.44 \pm 0.01$  ( $n = 1138$  female-nest-cell-years) and varied between  
306 years. Nest success rate was highest in 2012 ( $0.51 \pm 0.04$ ;  $n = 123$  female-nest-cell-years) and lowest in

307 2019 ( $0.36 \pm 0.07$ ;  $n = 50$  female-nest-cell-years). We found no significant change in nest success rate  
308 over time (Table 3). However, our analysis of the full dataset (1994 – 2019) did find evidence of a longer-  
309 term increase in nest success rate. Most often cells contained only one nest from one female in a given  
310 year (80.84% female-nest-cell-years; range 1 – 4). As such, nest success rates were generally either 0.00  
311 (51.41%;  $n = 585$  female-nest-cell-years) or 1.00 (39.81%;  $n = 453$  female-nest-cell-years).

312

313 We found no effect of mean height on nest success rate (female-nest-cell-years in which nest success  
314 rate  $> 0.00$ :  $3.00 \pm 0.04$  m; female-nest-cell-years in which nest success rate was 0.00:  $3.02 \pm 0.03$  m;  
315 Table 3, Figure 4a–b). Similarly, we found no effect of SD height on nest success rate (Table 3).  
316 However, there was a significant decline in nest success rate with increasing groundstorey volume  
317 (female-nest-cell-years in which nest success rate  $> 0.00$ :  $463.96 \pm 11.39$  m<sup>3</sup>; female-nest-cell-years in  
318 which nest success rate was equal to 0.00:  $490.16 \pm 12.07$ ; Table 3, Figure 4c–d).

319

### 320 *Fledgling survival rate*

321 Fledgling survival rate was on average  $0.61 \pm 0.02$  ( $n = 556$  female-nest-cell-years). Fledgling survival  
322 rate was highest in 2016 ( $0.76 \pm 0.04$ ;  $n = 53$  female-nest-cell-years) and lowest in 2013 ( $0.50 \pm 0.05$ ;  
323  $n = 57$  female-nest-cell-years). The average number of fledglings produced across all female-nest-cell-  
324 years was  $2.96 \pm 0.05$  (range: 1 - 9).

325

326 None of the understorey vegetation structure parameters were significant as main effects for fledgling  
327 survival rate (Table 3). However, we did find a significant interaction between mean height and  
328 groundstorey volume: fledgling survival rates decreased with groundstorey volume when female-nest-  
329 cell-years contained smaller understorey vegetation (when mean height was lower than the population-  
330 level average,  $n = 268$  female-nest-cell-years; Table 3, Figure 5).

331

## 332 **DISCUSSION**

333 Our study combined ALS-derived measures of understorey vegetation structure with breeding data  
334 from a long-term study of a population of superb fairy-wrens. We found differences in the  
335 characteristics of understorey vegetation structure in sites chosen for nesting, but no evidence that this  
336 selection reduced rates of nest or fledgling predation. We discuss the outcomes of these results below,

337 and the implications for the use of ALS in studies of the evolutionary and behavioural ecology of wild  
338 animal populations.

339

#### 340 *Understorey vegetation structure characteristics and nest-site selection*

341 Our results show that female superb fairy-wrens select nest-sites based on aspects of the understorey  
342 vegetation. Nest presence increased with decreasing mean height of the understorey vegetation and  
343 with groundstorey volume, which is indicative of an area containing more grass tussocks and small  
344 shrubs, substrates preferentially used in our study area by superb fairy-wrens for nesting (Figure S2).  
345 We found no statistical significance of SD height affecting the probability of nest presence in our main  
346 analysis, using data from 2009 – 2019. However, there was statistical support for the positive  
347 association between SD height and nest presence in our analysis of the full dataset (1994 – 2019),  
348 suggesting that there is a potential role for vegetation complexity in nest-site selection in superb fairy-  
349 wrens. Denser and more complex vegetation is expected to be favoured in response to visually and  
350 auditorily-oriented predators (Bowman & Harris, 1980; Martin, 1993; Martin & Roper, 1988; Filliater  
351 et al., 1994). Our results are therefore consistent with the expectation that superb fairy-wrens' choice of  
352 nest-site is shaped by predation pressures.

353

#### 354 *Understorey vegetation structure characteristics and breeding performance*

355 Despite the observation of preference for nest-sites with denser vegetation, our study using ALS data  
356 confirmed previous, somewhat counterintuitive, findings that nest success and fledgling survival rates  
357 of superb fairy-wrens decrease with increasing vegetation density (Backhouse et al., 2023; Colombelli-  
358 Négrel & Kleindorfer, 2009) at a height relevant to this species. These findings contradict the  
359 expectation that dense vegetation should be adaptive against visually and auditorily-oriented predators,  
360 such as pied currawongs. We suggest several possible explanations for this paradox.

361

362 Although pied currawongs were previously identified as the dominant predator of superb fairy-wren  
363 nests and fledglings in our study population (Prawiradilaga, 1996), they were not present in our study  
364 area until the 1970s (Taylor, 1992). Thus, superb fairy-wren nest-site selection likely evolved in response  
365 to historical selection pressures from different predatory species (Chalfoun & Schmidt, 2012). It is  
366 therefore possible that current nest-site preferences are insufficient at impeding the pied currawong's  
367 ability to detect and access the nests and fledglings of superb fairy-wrens. Alternatively, superb fairy-

368 wren nest-site selection might be adaptive against pied currawongs, but the current importance of pied  
369 currawongs as a predator may have been overestimated or have changed in recent years, since  
370 Prawiradilaga (1996). There is some support for this notion in the fact that despite an increase in the  
371 number of pied currawongs in our study area (A. Cockburn, unpublished data), long-term rates of  
372 superb fairy-wren nest predation have decreased (Table S1; Backhouse et al., 2023).

373

374 It is also possible that nesting in areas with increased groundstorey volume may make superb fairy-  
375 wren nests and fledglings more vulnerable to other predators (Filliater et al., 1994), such as red foxes  
376 *Vulpes vulpes*, which are common predators of superb fairy-wren nests and fledglings in our study area  
377 (R.S. Turner, unpublished data). Red foxes have been linked to the extinction of native species and  
378 population declines elsewhere throughout Australia because of their generalist diet and ability to thrive  
379 in various habitats (Woinarski et al. 2019, 2022). Moreover, they often locate their prey using olfactory  
380 cues, which may not be reduced by structural vegetation characteristics (Colombelli-Négrel &  
381 Kleindorfer, 2009). We do not have sufficient observations of predation events to determine if the  
382 importance of understorey vegetation structure impacts superb fairy-wren breeding performance  
383 differently depending on the predator, but our results illustrate the need to understand the potential  
384 importance of other predators.

385

### 386 *Potential use and limitations of ALS in evolutionary and behavioural ecology*

387 Studies have demonstrated the effectiveness of using ALS-derived measurements to assess  
388 relationships between vegetation structure and the abundance, richness, and distribution of different  
389 species (Ciuti et al., 2017; Davies & Asner, 2014; de Vries et al., 2021; Moudrý et al., 2023; Shokirov et  
390 al., 2023). More recently, some studies have also shown that ALS can be used to assess how structural  
391 vegetation characteristics affect breeding behaviours and life-histories of single populations or species  
392 (Davies et al., 2016, 2019; Hill et al., 2004; Hill & Hinsley, 2015; Klein et al., 2020). However, to date  
393 these studies have been largely limited to specific regions – in particular, North America and Europe –  
394 and taxonomic groups (Davies & Asner, 2014). With the increasing accessibility of national and regional  
395 ALS datasets (Kissling et al., 2022; Lefsky et al. 2002; Moudrý et al., 2023; Vierling et al. 2008) global  
396 studies for entire taxonomic groups and ecosystems are now possible, and with them the potential to  
397 significantly improve our understanding of animal-habitat relationships.

398

399 Compared to traditional manual methods of measuring vegetation structure (Block et al., 1987; Gotfryd  
400 & Hansell, 1985; MacArthur & MacArthur, 1961) ALS is overall less costly, less labour intensive, and  
401 less subjective. ALS also allows for data collection in remote or inaccessible areas, and over larger spatial  
402 extents, and can produce high-resolution measures of vegetation structure that are more representative  
403 of the broader landscape (though previous studies have found positive associations between structural  
404 vegetation characteristics derived from ALS and those measured in the field; Hyde et al., 2005, 2006).  
405 Additionally, ALS allows for more complex measures of vegetation structure to be calculated (Bakx et  
406 al., 2019), which can be updated as our understanding improves.

407  
408 Despite its potential, ALS has some limitations. First, data can be computationally demanding and  
409 require a significant amount of memory (Kissling et al., 2022; Vo et al., 2016). The unprocessed ALS  
410 data for our comparatively small study area was c. 10 GB in size and initially consisted of c. 250 million  
411 data points. Additionally, processing, and analysing ALS data requires a certain level of specialisation.  
412 However, there has been considerable development in the field of available software that has made  
413 processing and analysing ALS data more accessible (Kissling et al., 2022; Roussel et al., 2020; van Rees,  
414 2013). Second, ALS surveys are often conducted in winter, during leaf-off conditions for deciduous  
415 species, as their primary function is generally to provide accurate mapping of the ground terrain  
416 (Reutebuch et al., 2005). Future studies are needed to understand the effect of seasonality on the ability  
417 of ALS to capture structural data, particularly in landscapes with abundant deciduous species. In our  
418 study area, the vegetation is predominantly evergreen (Fraser & Purdie, 2020). Third, ALS may be less  
419 effective at capturing structural characteristics of understory vegetation in landscapes with dense  
420 canopy coverage (Bakx et al., 2019), particularly when point clouds are of a low density. However, a  
421 recent study by Shokirov et al. (2023) showed that ALS can effectively capture understory vegetation  
422 in similar landscapes to our study area, which has an open canopy, when compared to higher-resolution  
423 Terrestrial Laser Scanning (TLS) data. Moreover, several other studies have shown that estimating  
424 vegetation structure at coarser resolution of 20 – 25 m can be sufficient at reducing potential errors in  
425 sampling due to low point cloud density (Ruiz et al., 2014; Treitz et al., 2012; Wilkes et al., 2015).

426

## 427 **CONCLUSION**

428 Our study used ALS to investigate breeding behaviour in a wild superb fairy-wren population and found  
429 that aspects of understory vegetation structure played a role in nest-site selection. However,

430 relationships between understorey vegetation structure and breeding performance were complex and  
431 our findings highlighted the need for future research to consider the importance of specific predators.  
432 The increasing availability of ALS data offers potential for obtaining more complex, and less subjective,  
433 measures of vegetation structure for use in furthering our understanding the ecological pressures that  
434 shape breeding behaviours and life-histories of wild animals.

435

#### 436 **ACKNOWLEDGEMENTS**

437 We thank Andrew Cockburn for the superb fairy-wren breeding dataset and for discussion and  
438 comments on the manuscript. We also thank Fiona Backhouse for useful discussion during the  
439 conceptualisation of this project, and to the many field assistants who have contributed to the long-term  
440 study over the years. We thank the Australian National Botanic Gardens for permission to work at the  
441 study site (Permit Number: 2013/14-1) and for logistical support, and to the Australian Research  
442 Council for long-term funding, of which the latest grant for data used in this study was DP190100424  
443 to Loeske E. B. Kruuk, Andrew Cockburn, and Martijn van de Pol. We also thank two anonymous  
444 reviewers for helpful comments on the manuscript. Richard S. Turner was funded through an Australian  
445 National University Research Scholarship (7382018) and HDR Fee Merit Scholarship (3202015) and  
446 Loeske E. B. Kruuk was funded by an Australian Research Council Laureate Fellowship (FL200100068)  
447 and a Royal Society Research Professorship. Ethics approval was granted by the Australian National  
448 University Animal Experimentation Ethics Committee (Protocol Number: A2019/23). We wish to  
449 acknowledge the Ngunnawal people, the traditional custodians of the land upon which our study was  
450 undertaken. We pay our respects to their Elders, past, present, and emerging.

451

#### 452 **CONFLICT OF INTEREST**

453 The authors declare no conflict(s) of interest.

454

#### 455 **AUTHOR CONTRIBUTIONS**

456 Project conceptualisation: RST, OJDL, KNY, SS, LEBK; Airborne Laser Scanning data processing: RST,  
457 OJDL, KNY, SS; Superb fairy-wren data collection and management: HLO; Statistical analysis: RST;  
458 Original draft of manuscript: RST; Editing and review of manuscript: RST, KNY, LEBK. All authors gave  
459 approval of final manuscript.

460



461 **DATA SHARING**

462 Data needed to evaluate the conclusions presented in this study have been deposited at  
463 <https://doi.org/10.6084/m9.figshare.21743402> and will be publicly available following peer-review.

464

465 **REFERENCES**

466 Backhouse, F., Osmond, H.L., Doran, B., Stein, J., Kruuk, L.E.B., & Cockburn, A. (2023). Population  
467 decline reduces cooperative breeding in a spatially heterogenous population of superb fairy-wrens.  
468 *EcoEvoRxiv*, <https://doi.org/10.32942/X2FG6R>.

469 Bakx, T.R.M., Koma, Z., Seijmonsbergen, A.C., & Kissling, W.D. (2019). Use and categorisation of light  
470 detection and ranging vegetation metrics in avian diversity and species distribution research. *Diversity*  
471 *and Distributions*, *25*, 1045–1059.

472 Bayly, K.L., & Blumstein, D.T. (2001). Pied currawongs and the decline of native birds. *Emu*, *101*, 199–  
473 204.

474 Béland, M., Baldocchi, D.D., Widlowski, J.L., Fournier, R.A., & Verstraete, M.M. (2014). On seeing the  
475 wood from the leaves and the role of voxel size in determining leaf area distribution of forests with  
476 terrestrial LiDAR. *Agricultural and Forest Meteorology*, *184*, 82–97.

477 Block, W.M., With, K.A., & Morrison, M.L. (1987). On measuring bird habitat: Influence of observer  
478 variability and sample size. *The Condor*, *89*, 241–251.

479 Borgmann, K.L., & Conway, C.J. (2015). The nest-concealment hypothesis: New insights from a  
480 comparative analysis. *The Wilson Journal of Ornithology*, *127*, 646–660.

481 Bowman, G.B., & Harris, L.D. (1980). Effect of spatial heterogeneity on ground-nest depredation. *The*  
482 *Journal of Wildlife Management*, *44*, 806–813.

483 Bürkner, P.C. (2017). brms: An R package for Bayesian multilevel models using Stan. *Journal of*  
484 *Statistical Software* *80*, 1–28.

485 Chalfoun, A.D., & Schmidt, K.A. (2012). Adaptive breeding-habitat selection: Is it for the birds? *The*  
486 *Auk*, *129*, 589–599.

- 487 Ciuti, S., Tripke, H., Antkowiak, P., Gonzalez, R.S., Dormann, C.F., & Heurich, M. (2017). An efficient  
488 method to exploit LiDAR data in animal ecology. *Methods in Ecology and Evolution*, 9, 893–904.
- 489 Cockburn, A., Brouwer, L., Margraf, N., Osmond, H.L. & van de Pol, M. (2016). Superb fairy-wrens:  
490 Making the worst of a good job. In: Koenig, W.D. & Dickinson, J.L. (Eds). *Cooperative Breeding in*  
491 *Vertebrates: Studies of Ecology, Evolution, and Behaviour*, pp. 133–149. Cambridge University Press,  
492 Cambridge, UK.
- 493 Cockburn, A., Sims, R.A., Osmond, H.L., Green, D.J., Double, M.C., & Mulder, R.A. (2008). Can we  
494 measure the benefits of help in cooperatively breeding birds: The case of superb fairy-wrens *Malurus*  
495 *cyaneus*? *Journal of Animal Ecology*, 77, 430–438.
- 496 Collier, P., & Steed, J. (2001). Australia's national GDA94 transformation grids. In *42nd Australian*  
497 *Surveyors Congress, Brisbane, Australia*.
- 498 Colombelli-Négrel, D., & Kleindorfer, S. (2009). Nest height, nest concealment, and predator type  
499 predict nest predation in superb fairy-wrens (*Malurus cyaneus*). *Ecological Research*, 24, 921–928.
- 500 Cooper, E.B., Bonnet, T., Osmond, H.L., Cockburn, A., & Kruuk, L.E.B. (2020). Do the ages of parents  
501 or helpers affect offspring fitness in a cooperatively breeding bird? *Journal of Evolutionary*  
502 *Biology*, 33, 1735–1748.
- 503 Davies, A.B., & Asner, G.P. (2014). Advances in animal ecology from 3D-LiDAR ecosystem mapping.  
504 *Trends in Ecology & Evolution*, 29, 681–691.
- 505 Davies, A.B., Marneweck, D.G., Druce, D.J., & Asner, G.P. (2016). Den site selection, pack composition,  
506 and reproductive success in endangered African wild dogs. *Behavioural Ecology*, 27, 1869–1879.
- 507 Davies, A.B., Oram, F., Ancrenaz, M., & Asner, G.P. (2019). Combining behavioural and LiDAR data to  
508 reveal relationships between canopy structure and orangutan nest site selection in disturbed forests.  
509 *Biological Conservation*, 232, 97–107.
- 510 de Vries, J.P.R., Koma, Z., de Vries, M.F.W., & Kissling, W.D. (2021). Identifying fine-scale habitat  
511 preferences of threatened butterflies using airborne laser scanning. *Diversity and Distributions*, 27,  
512 1251–1264.

- 513 Dormann, C.F., Elith, J., Bacher, S., Buchmann, C., Carl, G., Carré, G., Marquéz, J.R.G., Gruber, B.,  
514 Lafourcade, B., Leitão, P.J., Münkemüller, T., McClean, C., Osborne, P.E., Reineking, B., Schröder, B.,  
515 Skidmore, A.K., Zurell, D., & Lautenbach, S. (2013). Collinearity: A review of methods to deal with it  
516 and a simulation study evaluating their performance. *Ecography*, *36*, 27–46.
- 517 Dormann, C.F., McPherson, J.M., Araújo, M.B., Bivand, R., Bolliger, J., Carl, G., Davies, R.G., Hirzel,  
518 A., Jetz, Kissling, W.D., Kühn, I., Ohlemüller, R., Peres-Neto, P.R., Reineking, B., Schröder, B., Schurr,  
519 F.M., & Wilson, R. (2007). Methods to account for spatial autocorrelation in the analysis of species  
520 distributional data: A review. *Ecography*, *30*, 609–628.
- 521 Filliater, T.S., Breitwisch, R., & Nealen, P.M. (1994). Predation on northern cardinal nests: Does choice  
522 of nest site matter? *The Condor*, *96*, 761–768.
- 523 Fulton, G.R. (2019). Meta-analyses of nest predation in temperate Australian forests and woodlands.  
524 *Austral Ecology*, *44*, 389–396.
- 525 Fulton, G.R., & Ford, H.A. (2001). The pied currawong's role in avian nest predation: A predator  
526 removal experiment. *Pacific Conservation Biology*, *7*, 154–160.
- 527 Fraser, I., & Purdie, R. (2020). Black Mountain: A natural history of a Canberra icon. Friends of Black  
528 Mountain, Canberra, Australia.
- 529 Gabry, J., & Mahr, T. (2021). bayesplot: Plotting for Bayesian models. R package version 1.8.1. Available  
530 from: <https://mc-stan.org/bayesplot>.
- 531 Gelman, A., Carlin, J.B., Stern, H.S., Dunson, D.B., Vehtari, A., & Rubin, D.B. (2013). Bayesian data  
532 analysis (3rd edition). Chapman & Hall/CRC Press, London, UK.
- 533 Gelman, A., Lee, D. & Guo, J. (2015). Stan: A probabilistic programming language for Bayesian  
534 inference and optimization. *Journal of Educational and Behavioural Statistics*, *40*, 530–543.
- 535 Gotfryd, A., & Hansell, R.I.C. (1985). The impact of observer bias on multivariate analyses of vegetation  
536 structure. *Oikos*, *45*, 223–234.
- 537 Hajduk, G.K., Cockburn, A., Margraf, N., Osmond, H.L., Walling, C.A., & Kruuk, L.E.B. (2018).  
538 Inbreeding, inbreeding depression, and infidelity in a cooperatively breeding bird. *Evolution*, *72*, 1500–  
539 1514.

- 540 Hajduk, G.K., Walling, C.A., Cockburn, A., & Kruuk, L.E.B. (2020). The 'algebra of evolution': The  
541 Robertson-Price identity and viability selection for body mass in a wild bird population. *Philosophical  
542 Transactions of the Royal Society B: Biological Sciences*, 375, 20190359.
- 543 Hajduk, G.K., Cockburn, A., Osmond, H.L. & Kruuk, L.E.B. (2021). Complex effects of helper  
544 relatedness on female extrapair reproduction in a cooperative breeder. *Behavioural Ecology*, 32, 386–  
545 394.
- 546 Harrison, X.A., Donaldson, L., Correa-Cano, M.E., Evans, J., Fisher, D.N., Goodwin, C.E.D., Robinson,  
547 B.S., Hodgson, D.J., & Inger, R. (2018). A brief introduction to mixed effects modelling and multi-model  
548 inference in ecology. *Peer J*, 6, 1–32.
- 549 Hill, R.A., & Hinsley, S.A. (2015). Airborne LiDAR for woodland habitat quality monitoring: Exploring  
550 the significance of LiDAR data characteristics when modelling organism-habitat relationships. *Remote  
551 Sensing*, 7, 3446–3466.
- 552 Hill, R.A., Hinsley, S.A., Gaveau, D.L.A., & Bellamy, P.E. (2004). Cover: Predicting habitat quality for  
553 great tits (*Parus major*) with airborne laser scanning data. *International Journal of Remote Sensing*,  
554 25, 4851–4855.
- 555 Hyde, P., Dubayah, R., Peterson, B., Blair, J.B., Hofton, M., Hunsaker, C., & Walker, W. (2005).  
556 Mapping forest structure for wildlife habitat analysis using waveform LiDAR: Validation of montane  
557 ecosystems. *Remote sensing of Environment*, 96, 427–437.
- 558 Hyde, P., Dubayah, R., Walker, W., Blair, J.B., Hofton, M., & Hunsaker, C. (2006). Mapping forest  
559 structure for wildlife habitat analysis using multi-sensor (LiDAR, SAR/InSAR, ETM+, Quickbird)  
560 synergy. *Remote Sensing of Environment*, 102, 63–73.
- 561 Ibáñez-Álamo, J.D., Magrath, R.D., Oteyza, J.C., Chalfoun, A.D., Haff, T.M., Schmidt, K.A., Thomson,  
562 R.L., & Martin, T.E. (2015). Nest predation research: Recent findings and future perspectives. *Journal  
563 of Ornithology*, 156, 247–262.
- 564 Klein, J., Haverkamp, P.J., Lindberg, E., Griesser, M., & Eggers, S. (2020). Remotely sensed forest  
565 understory density and nest predator occurrence interact to predict suitable breeding habitat and the  
566 occurrence of a resident boreal bird species. *Ecology and Evolution*, 10, 2238–2252.

- 567 Koma, Z., Grootes, M.W., Meijer, C.W., Nattino, F., Seijmonsbergen, A.C., Sierdsema, H., Foppen, R.,  
568 & Kissling, W.D. (2021). Niche separation of wetland birds revealed from airborne laser scanning.  
569 *Ecography*, 44, 907–918.
- 570 Kruuk, L.E.B., Osmond, H.L., & Cockburn, A. (2015). Contrasting effects of climate on juvenile body  
571 size in a Southern Hemisphere passerine bird. *Global Change Biology*, 21, 2929–2941.
- 572 Kubelka, V., Šálek, M., Tomkovich, P., Végvári, Z., Freckleton, R.P., & Székely, T. (2018). Global pattern  
573 of nest predation is disrupted by climate change in shorebirds. *Science*, 362, 680–683.
- 574 Lahti, D.C. (2009). Why we have been unable to generalise about bird nest predation. *Animal*  
575 *Conservation*, 12, 279–281.
- 576 Lefsky, M.A., Cohen, W.B., Parker, G.G., & Harding, D.J. (2002). LiDAR remote sensing for ecosystem  
577 studies: LiDAR, an emerging remote sensing technology that directly measures the three-dimensional  
578 distribution of plant canopies, can accurately estimate vegetation structural attributes and should be of  
579 particular interest to forest, landscape, and global ecologists. *BioScience*, 52, 19–30.
- 580 Lima, S.L. (2009). Predators and the breeding bird: Behavioural and reproductive flexibility under the  
581 risk of predation. *Biological Reviews*, 84, 485–513.
- 582 Lima, S.L., & Dill, L.M. (1990). Behavioural decisions made under the risk of predation: A review and  
583 prospectus. *Canadian Journal of Zoology*, 68, 619–640.
- 584 Lv, L., Yang L., Osmond, H.L., Cockburn, A. & Kruuk, L.E.B. (2019). When to start and when to stop:  
585 Effects of climate on breeding in a multi-brooded songbird. *Global Change Biology*, 26, 443–457.
- 586 Lv, L., van de Pol, M., Osmond, H.L., Liu, Y., Cockburn, A., & Kruuk, L.E.B. (2023). Winter mortality of  
587 a passerine bird increases following hotter summers and during winters with higher maximum  
588 temperatures. *Science Advances*, 9, eabm019.
- 589 MacArthur, R.H., & MacArthur, J.W. (1961). On bird species diversity. *Ecology*, 42, 594–598.
- 590 Magrath, R.D., Haff, T.M., Horn, A.G., & Leonard, M.L. (2010). Calling in the face of danger: Predation  
591 risk and acoustic communication by parent birds and their offspring. In: Brockmann, H. J., Roper, T.  
592 J., Naguib, M., Wynne-Edwards, K. E., Mitani, J. C., & Simmons, L. W. (Eds.), *Advances in the Study of*  
593 *Behaviour*, pp. 187–253. Academic Press, London, UK.

- 594 Martin, T.E. (1993). Nest predation and nest sites. *BioScience*, *43*, 523–532.
- 595 Martin, T.E., & Roper, J.J. (1988). Nest predation and nest-site selection of a western population of the  
596 hermit thrush. *The Condor*, *90*, 51–57.
- 597 Matysioková, B., & Remeš, V. (2022). Stronger negative species interactions in the tropics supported by  
598 a global analysis of nest predation in songbirds. *Journal of Biogeography*, *49*, 511–522.
- 599 Moudrý, V., Cord, A.F., Gábor, L., Laurin, G.V., Barták, V., Gdulová, K., Malavasi, M., Rocchini, D.,  
600 Stereńczak, K., Prošek, J., & Wild, J. (2023). Vegetation structure derived from airborne laser scanning  
601 to assess species distribution and habitat suitability: The way forward. *Diversity and Distributions*, *29*,  
602 39–50.
- 603 Mouton, J.C., & Martin, T.E. (2019). Nest structure affects auditory and visual detectability, but not  
604 predation risk, in a tropical songbird community. *Functional Ecology*, *33*, 1973–1981.
- 605 Naef-Daenzer, B., & Gruebler, M.U. (2016). Post-fledging survival of altricial birds: Ecological  
606 determinants and adaptation. *Journal of Field Ornithology*, *87*, 227–250.
- 607 Naef-Daenzer, B., Widmer, F., & Nuber, M. (2001). Differential post-fledging survival of great and coal  
608 tits in relation to their condition and fledging date. *Journal of Animal ecology*, *70*, 730–738.
- 609 Prawiradilaga, D. M. (1996). Foraging ecology of pied currawongs *Strepera graculina* in recently  
610 colonised areas of their range [PhD Thesis]. Australian National University.
- 611 R Core Team (2021). R: A language and environment for statistical computing. R Foundation for  
612 Statistical Computing, Vienna, Austria.
- 613 Remeš, V., Matysioková, B., & Cockburn, A. (2012a). Long-term and large-scale analyses of nest  
614 predation patterns in Australian songbirds and a global comparison of nest predation rates. *Journal of*  
615 *Avian Biology*, *43*, 435–444.
- 616 Remeš, V., Matysioková, B., & Cockburn, A. (2012b). Nest predation in New Zealand songbirds: Exotic  
617 predators, introduced prey and long-term changes in predation risk. *Biological Conservation*, *148*, 54–  
618 60.
- 619 Reutebuch, S.E., Andersen, H.E., & McGaughey, R.J. (2005). Light detection and ranging (LIDAR): An  
620 emerging tool for multiple resource inventory. *Journal of Forestry*, *103*, 286–292.

- 621 Ricklefs R.E. (1969). An analysis of nesting mortality in birds. *Contributions to Zoology*, 9, 1–48.
- 622 Roussel, J.R., Auty, D., Coops, N.C., Tompalski, P., Goodbody, T.R.H., Sánchez Meador, A., Bourdon,  
623 J.F., De Boissieu, F. & Achim, A. (2020). lidR: An R package for analysis of Airborne Laser Scanning  
624 (ALS) data. *Remote Sensing of Environment*, 251, 112061.
- 625 Rowley, I. & Russell, E.M. (1997). Fairy-wrens and grasswrens: Maluridae. Oxford University Press,  
626 Oxford, UK.
- 627 Ruiz, L.A., Hermosilla, T., Mauro, F., & Godino, M. (2014). Analysis of the influence of plot size and  
628 LiDAR density on forest structure attribute estimates. *Forests*, 5, 936–951.
- 629 Sasaki, T., Imanishi, J., Fukui, W., & Morimoto, Y. (2016). Fine-scale characterization of bird habitat  
630 using airborne LiDAR in an urban park in Japan. *Urban Forestry and Urban Greening*, 17, 16–22.
- 631 Schielzeth, H. (2010). Simple means to improve the interpretability of regression coefficients. *Methods*  
632 *in Ecology and Evolution*, 1, 103–113.
- 633 Schlotfeldt, B., & Kleindorfer, S. (2006). Adaptive divergence in the superb fairy-wren (*Malurus*  
634 *cyaneus*): A mainland versus island comparison of foraging behaviour, morphology, and vegetation.  
635 *Emu-Austral Ornithology*, 106, 309–319.
- 636 Shokirov, S. (2021). Using multi-platform LiDAR to assess vegetation structure for woodland forest  
637 fauna [PhD Thesis]. Australian National University.
- 638 Shokirov, S., Jucker, T., Levick, S.R., Manning, A.D., Bonnet, T., Yebra, M., & Youngentob, K.N. (2023).  
639 Habitat highs and lows: Using terrestrial and UAV LiDAR for modelling avian species richness and  
640 abundance in a restored woodland. *Remote Sensing of Environment*, 285, 113326.
- 641 Stoker, J. (2009). Visualization of multiple-return LiDAR data: Using voxels. *Photogrammetric*  
642 *Engineering and Remote Sensing*, 75, 109–112.
- 643 Taylor, C.J., & Langmore, N.E. (2020). How do brood-parasitic cuckoos reconcile conflicting  
644 environmental and host selection pressures on egg size investment? *Animal Behaviour*, 168, 89–96.
- 645 Taylor, M. (1992). Birds of the Australian Capital Territory: An Atlas. Canberra Ornithologists Group  
646 and National Capital Planning Authority, Canberra, Australia.

- 647 Treitz, P., Lim, K., Woods, M., Pitt, D., Nesbitt, D., & Etheridge, D. (2012). LiDAR sampling density for  
648 forest resource inventories in Ontario, Canada. *Remote Sensing*, 4, 830–848.
- 649 van Rees, E. (2013). Rapidlasso: Efficient tools for LiDAR processing. *GeoInformatics*, 16, 14–16.
- 650 Vehtari, A., Gelman, A., Simpson, D., Carpenter, B., & Bürkner, P.C. (2021). Rank-normalization,  
651 folding, and localisation: An improved R-hat for assessing convergence of MCMC (with discussion).  
652 *Bayesian Analysis*, 16, 667–718.
- 653 Vierling, K.T., Swift, C.E., Hudak, A.T., Vogeler, J.C., & Vierling, L.A. (2014). How much does the time  
654 lag between wildlife field-data collection and LiDAR-data acquisition matter for studies of animal  
655 distributions? A case study using bird communities. *Remote sensing letters*, 5, 185-193.
- 656 Vierling, K.T., Vierling, L.A., Gould, W.A., Martinuzzi, S., & Clawges, R.M. (2008). Lidar: Shedding new  
657 light on habitat characterization and modelling. *Frontiers in Ecology and the Environment*, 6, 90–98.
- 658 Vo, A.V., Laefer, D.F., & Bertolotto, M. (2016). Airborne laser scanning data storage and indexing:  
659 State-of-the-art review. *International Journal of Remote Sensing*, 37, 6187–6204.
- 660 Wilkes, P., Jones, S. D., Suarez, L., Haywood, A., Woodgate, W., Soto-Berelov, M., Mellor, A.,  
661 & Skidmore, A.K. (2015). Understanding the effects of ALS pulse density for metric retrieval across  
662 diverse forest types. *Photogrammetric Engineering & Remote Sensing*, 81, 625–635.
- 663 Woinarski, J.C., Braby, M.F., Burbidge, A.A., Coates, D., Garnett, S.T., Fensham, R.J., Legge, S.M.,  
664 McKenzie, N.L., Silcock, J.L., & Murphy, B. P. (2019). Reading the black book: The number, timing,  
665 distribution and causes of listed extinctions in Australia. *Biological Conservation*, 239, 108261.
- 666 Woinarski, J.C., Stobo-Wilson, A.M., Crawford, H.M., Dawson, S.J., Dickman, C.R., Doherty, T.S.,  
667 Fleming, P.A., Garnett, S.T., Gentle, M.N., Legge, S.M., Newsome, T.M., Palmer, R., Rees, M.W.,  
668 Ritchie, E.G., Speed, J., Stuart, J.M., Thompson, E., Turpin, J., & Murphy, B.P. (2022). Compounding  
669 and complementary carnivores: Australian bird species eaten by the introduced European red fox  
670 *Vulpes vulpes* and domestic cat *Felis catus*. *Bird Conservation International*, 32, 506–522.
- 671 Wood, K.A. (2000). Notes on the feeding habits of the pied currawong *Strepera graculina* at  
672 Wollongong, New South Wales. *Australian Bird Watcher*, 18, 259–266.



673 Yasukawa, K., & Cockburn, A. (2009). Antipredator vigilance in cooperatively breeding superb fairy-  
674 wrens (*Malurus cyaneus*). *The Auk*, 126, 147–154.

675 Zuur, A.F., Ieno, E.N., Walker, N.J., Saveliev, A.A., & Smith, G.M. (2009). Mixed effects models and  
676 extensions in ecology with R. Springer, New York, USA.

677

## 678 SUPPORTING INFORMATION

679 Additional supporting information may be found in the published version online in the Supporting  
680 Information section at the end of the article.

681 **Video S1.** Animation of height-normalized LiDAR point cloud data used in this study. Appendix S1.  
682 Supplementary methods. Assessing spatial autocorrelation of different understorey vegetation  
683 structure parameters.

684 **Figure S1.** The height (cm) at which superb fairy-wrens build their nests in the study area.

685 **Figure S2.** The percentage of superb fairy-wren nests built in different vegetation substrates in the  
686 study area (A) between 2009–2019; (B) between 1994–2019.

687 **Figure S3.** The fate of superb fairy-wren nests in the study area (A) between 2009–2019; (B) between  
688 1994–2019.

689 **Figure S4.** Mean (SE) daily mortality rate of superb fairy-wren fledglings until independence (A)  
690 between 2009–2019; (B) between 1994–2019.

691 **Figure S5.** Mean (SE) daily maximum and minimum temperature, and total rainfall for each year  
692 of the study between 2009–2019.

693 **Figure S6.** The change in (A) nest presence; (B) the number of breeding females in the study area over  
694 time.

695 **Figure S7.** Mean (SE) number of LiDAR vegetation points in each cell at 2 m height increments.

696 **Figure S8.** Density plots of Monte-Carlo simulated Moran's I statistics ( $n = 2000$  simulations) for (A)  
697 mean height; (B) SD height; and (C) groundstorey volume in each dataset.

698 **Figure S9.** Visualisation of the spatial weights matrix used in each of our three Bayesian spatial  
699 hierarchical generalised linear models.

700 **Figure S10.** Spatiotemporal distribution of superb fairywren nest-sites in the study area between  
701 2009–2019.

702 **Table S1.** Summaries of Bayesian spatial hierarchical generalised linear regression models using the  
703 full breeding dataset from 1994–2019.

704 **Table S2.** Checking for multicollinearity among model parameters.

705 **Table S3.** Pearson coefficients indicating the level of relationship between main effect parameters in  
706 each of the three Bayesian spatial hierarchical regression models: (A) nest presence; (B) nest success  
707 rate; (C) fledgling survival rate.

708 **Table S4.** Checking for spatial autocorrelation among understory vegetation structure parameters.

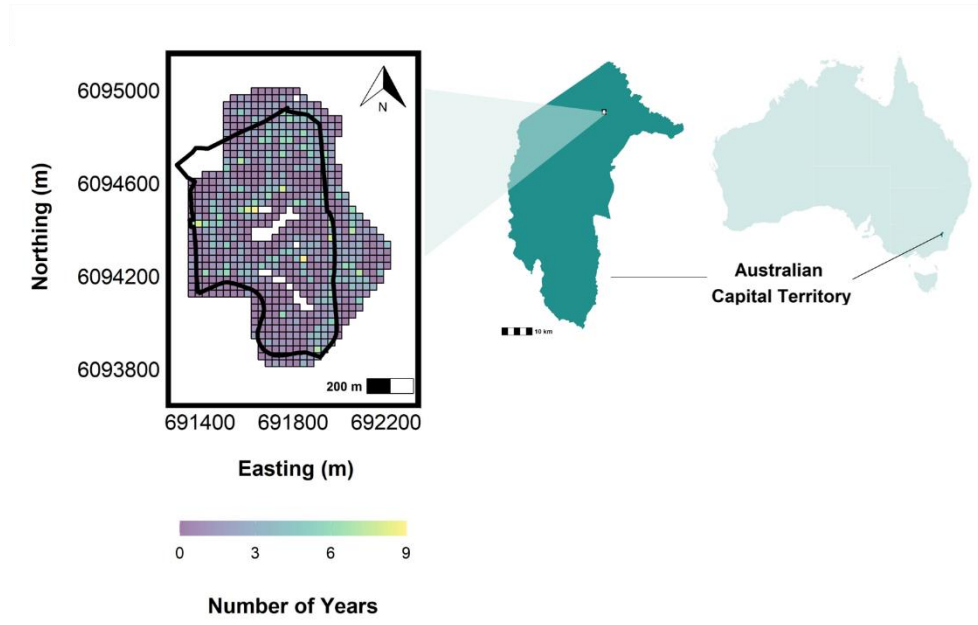


**Figure 1:** Location of the study area in Canberra, Australian Capital Territory, Australia. The study area encompasses an area of c. 65 hectares that includes a managed area (c. 43 hectares) in the Australian National Botanic Gardens (ANBG; the perimeter of which is shown in black) and an unmanaged area (c. 22 hectares), which is part of the adjacent Black Mountain Nature Reserve. We established a 30 x 30 m resolution grid ( $n = 768$  cells) over the extent of the study area, for which superb fairy-wren breeding data and ALS-derived vegetation structure parameters were extracted. Data for 27 of the 768 cells were excluded from analyses (shown in white), leaving a total of 741 cells (see main text for further details). The left-hand panel shows the spatial distribution of the 741 cells across the study area, with cells shaded based on the number of years they contained a nest-site; the middle panel shows the location of the study area within the Australian Capital Territory; and the right-hand panel shows the latter's location in Australia.

(a)

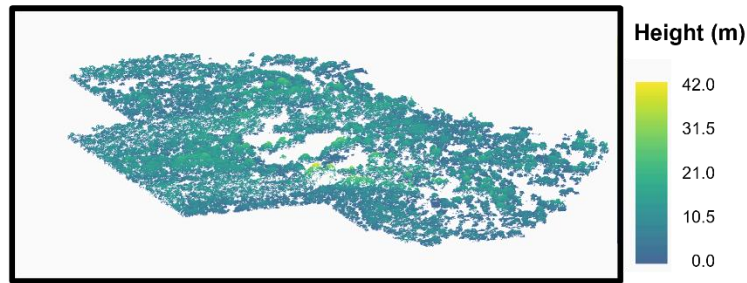
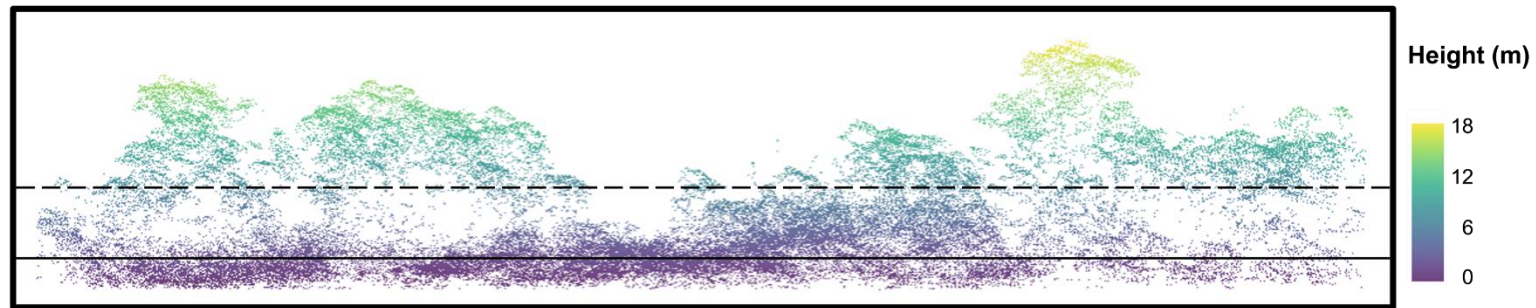


**Figure 2:** (a) Height-normalised LiDAR point cloud data for the study area acquired using ALS.

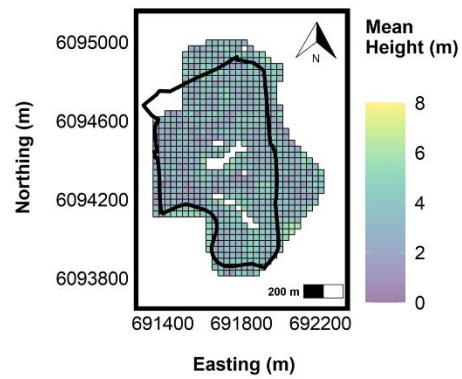
Note, ground points are not presented. A three-dimensional animation of these data is provided as Video S1. (b) An example 120 x 30 m cross-section of the point cloud data.

Dashed line indicates the cut-off point (8 m) between the understory and canopy layer. Solid line indicates the cut-off point (2 m) below which the groundstorey volume was estimated. (c - e) Spatial distribution of the three understory vegetation structure parameters used in the analysis (ANBG perimeter shown in black).

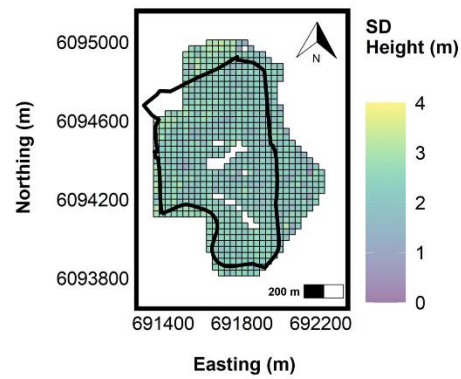
(b)



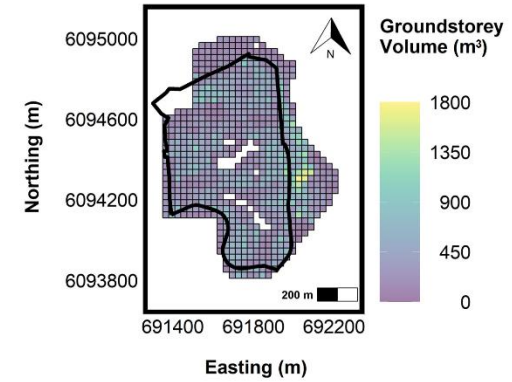
(c)



(d)



(e)



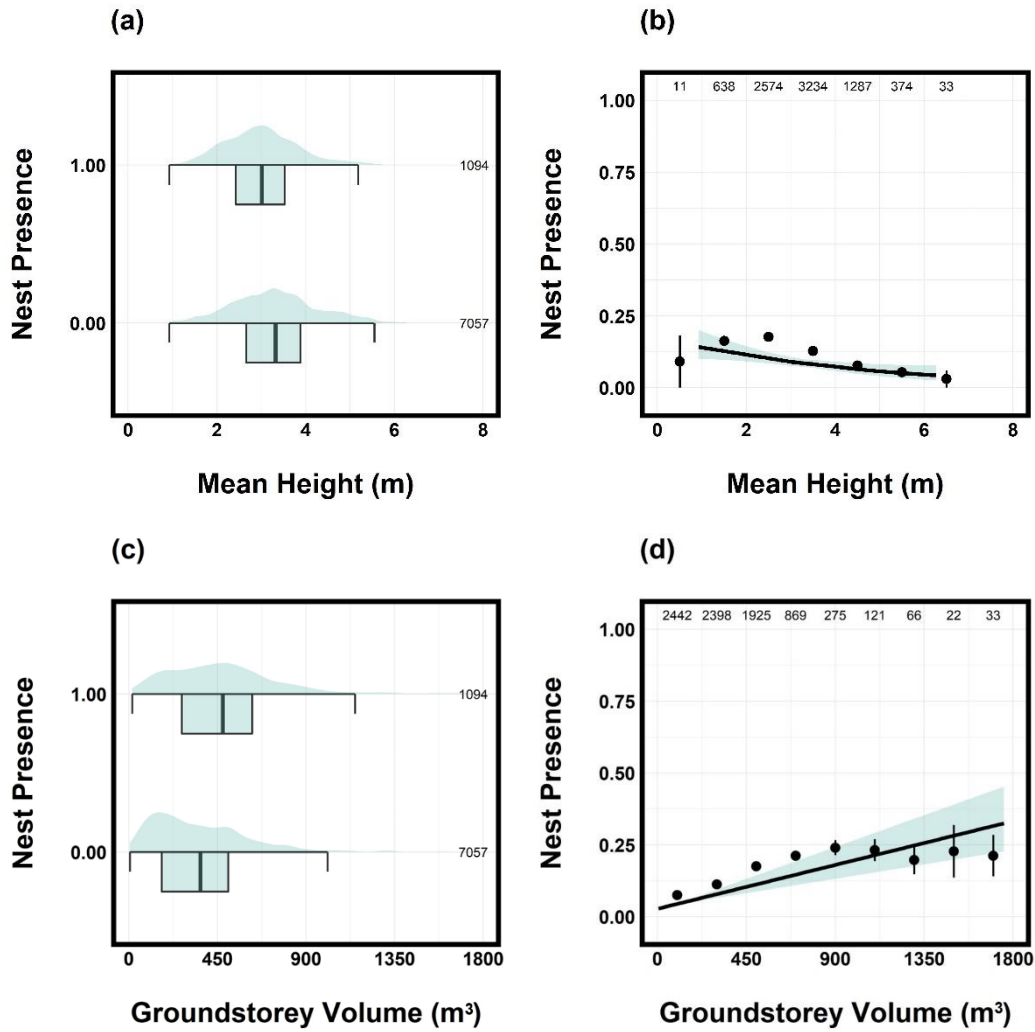


**Figure 3:** Nest presence in relation to (a – b) mean height and (c – d) groundstorey volume. Panels (a) and (c) show the distribution of the raw data. The box and whiskers show the mean, plus upper and lower quartiles, and the interquartile range of the raw data for each group. Panels (b) and (d) show the model estimated marginal means ( $\pm$  95% confidence intervals), after correcting for main effect parameters, as described in Methods. For visualisation purposes, the raw data were grouped into bins (each bin represents an interval of 1 m in (b) and an interval of 200 m<sup>3</sup> in (d)) with points showing the group mean  $\pm$  SE. In all panels, the number of observations (cell-years) in each group is given. Model estimates are provided in Table 3.

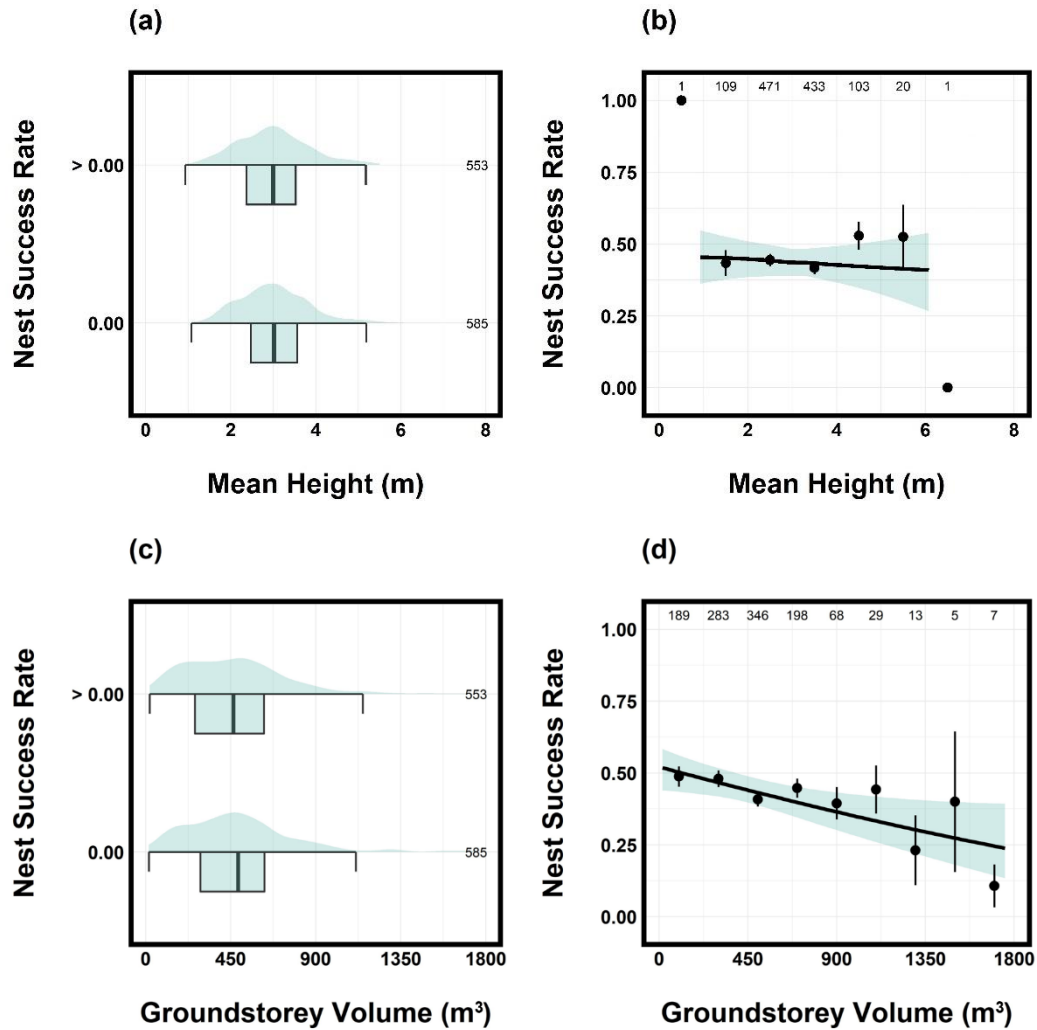


**Figure 4:** Nest success rate in relation to (a – b) mean height and (c – d) groundstorey volume. Panels (a) and (c) show the distribution of the raw data. For visualisation purposes, the raw data were grouped into two bins: 0.00 and > 0.00. The box and whiskers show the mean, plus upper and lower quartiles, and the interquartile range of the raw data for each group. Panels (b) and (d) show the model estimated marginal means ( $\pm$  95% confidence intervals), after correcting for main effect parameters, as described in Methods. For visualisation purposes, the raw data were grouped into bins (each bin represents an interval of 1 m in (b) and an interval of 200 m<sup>3</sup> in (d)) with points showing the group mean  $\pm$  SE. In all panels, the number of observations (female-nest-cell-years) in each group is given. Model estimates are provided in Table 3.

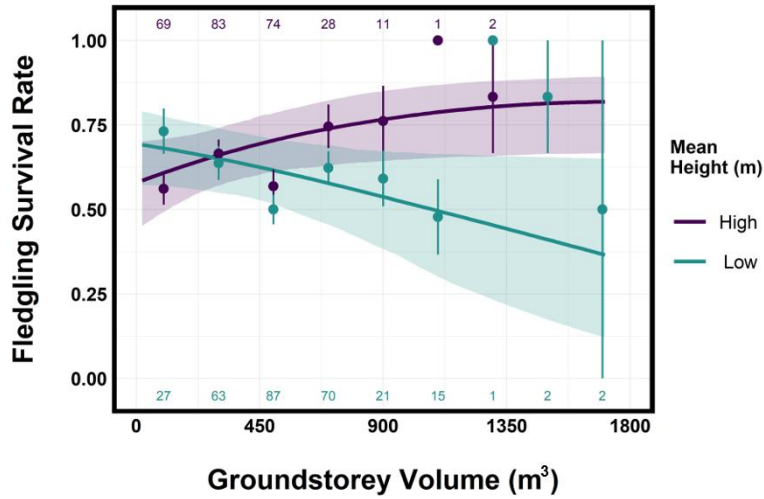


**Figure 5:** Fledgling survival rate in relation to groundstorey volume when vegetation is low (green; mean height is less than the population-level average) or high (purple; mean height is greater than the population-level average). Regression lines show the model estimated marginal means ( $\pm$  95% confidence intervals), after correcting for main effect parameters, as described in Methods. For visualisation purposes, the raw data were grouped into bins (each bin represents an interval of 200 m<sup>3</sup>) with points showing the group mean  $\pm$  SE. The number of observations (female-nest-cell-years) in each group is given. Model estimates are provided in Table 3.

**Table 1:** Definition of terms and overview of the superb fairy-wren breeding parameters used in this study.

Breeding Parameter	Observation Level	Number of Observations	Description	Model Structure
Nest Presence	A 30 x 30 m resolution cell in a given year (cell-year)	8151 cell-years (741 cells; 11 years)	Cells that contained a nest in a given year were assigned a binary score of 1 (nest-cell-year) otherwise 0 (unused cell-year)	Bernoulli error distribution (and logit-link function)
Nest Success Rate	A nest-cell for a given female in a given year (female-nest-cell-year)	1138 female-nest-cell-years	The number of successful nests relative to the total number of nest attempts for each female in a nest-cell in a given year	Binomial error distribution (and logit-link function). The denominator (the total number of nest attempts for each female-nest-cell-year) was equal to 1 in 80.8% of observations
Fledgling Survival Rate	A nest-cell for a given female in a given year (female-nest-cell-year)	556 female-nest-cell-years. Only female-nest-cell-years that contained one or more fledgling were included in this model	The number of fledglings to survive to independence relative to the total number of nestlings that successfully fledged for each female in a nest-cell in a given year	Binomial error distribution (and logit-link function). In total, 22.1% of observations were zeros. Therefore, to account for excess zeros in the Binomial error distribution, we included a zero-inflated parameter in this model (Bürkner, 2017)



**Table 2:** Overview of the understorey vegetation structure parameters derived from ALS for each 30 x 30 m resolution cell.  $z$  = normalised height value of LiDAR point; Voxel = A value of volume represented in three-dimensional ( $x, y, z$ ) space.

Parameter	Parameter Abbreviation	Height Threshold	Description	Ecological Interpretation
Mean height of the understorey vegetation (measured in metres)	Mean Height	0 – 8 m	Mean value of $z$ within each 30 x 30 m resolution cell	A high mean height value indicates that a cell contains more tall shrubs and small trees, and fewer grass tussocks. A low mean height value indicates that a cell contains more grass tussocks and small shrubs. The spatial distribution of mean height across the study area is shown in Figure 2c.
Standard deviation of the height of the understorey vegetation (measured in metres)	SD Height	0 – 8 m	SD of $z$ values within each 30 x 30 m resolution cell	SD height describes the variation in the vegetation height. A high SD height value indicates that a cell contains a more heterogenous, or complex, vegetation height distribution. The spatial distribution of SD height across the study area is shown in Figure 2d.
Volume of the vegetation in the lowest layer of the understorey (measured in cubic metres).	Groundstorey Volume	0 – 2 m	The number of 1 x 1 x 1 m voxels <sup>†</sup> between 0–2 m containing one or more vegetation point within each 30 x 30 m resolution cell. Maximum potential groundstorey volume is 1800 m <sup>3</sup> (30 x 30 x 2 m).	The density of vegetation in the lowest understorey layer. The spatial distribution of groundstorey volume across the study area is shown in Figure 2e.

<sup>†</sup> Note: ALS point cloud data were converted to 1 x 1 x 1 m voxels using the `voxelize_points` function in the package 'lidR' (v.3.1.3; Rousel et al., 2020) in R (v.4.0.5; R Core Team, 2021). The method of using voxels to estimate vegetation density followed e.g., Béland et al. (2014); Sasaki et al. (2016); Shokirov (2021), Shokirov et al. (2023); Stoker (2009).

**Table 3:** Summaries of Bayesian spatial hierarchical generalised linear regression models. The parameter estimates are presented as posterior means  $\pm$  standard deviation (SD) and 95% credible intervals (CI). All explanatory parameters were mean standardised for analysis. Main effect parameters for which the 95% CI do not overlap zero are highlighted in bold.

Parameters	Nest Presence Estimate $\pm$ SD [95% CI]	Nest Success Rate Estimate $\pm$ SD [95% CI]	Fledgling Survival Rate Estimate $\pm$ SD [95% CI]
Intercept	<b>-2.37 <math>\pm</math> 0.09 [-2.54 – -2.19]</b>	<b>-0.38 <math>\pm</math> 0.13 [-0.63 – -0.12]</b>	<b>1.17 <math>\pm</math> 0.24 [0.70 – 1.64]</b>
Year	<b>-0.28 <math>\pm</math> 0.07 [-0.43 – -0.13]</b>	0.04 $\pm$ 0.09 [-0.13 – 0.20]	0.05 $\pm$ 0.16 [-0.27 – 0.37]
Mean Height	<b>-0.24 <math>\pm</math> 0.09 [-0.41 – -0.08]</b>	-0.04 $\pm$ 0.09 [-0.21 – 0.13]	0.24 $\pm$ 0.15 [-0.06 – 0.54]
SD Height	0.10 $\pm$ 0.07 [-0.04 – 0.25]	-0.04 $\pm$ 0.07 [-0.18 – 0.10]	-0.19 $\pm$ 0.13 [-0.44 – 0.05]
Groundstorey Volume	<b>0.42 <math>\pm</math> 0.08 [0.26 – 0.57]</b>	<b>-0.20 <math>\pm</math> 0.07 [-0.33 – -0.06]</b>	0.07 $\pm$ 0.12 [-0.17 – 0.31]
Groundstorey Volume: Mean Height	0.07 $\pm$ 0.07 [-0.06 – 0.20]	0.02 $\pm$ 0.07 [-0.11 – 0.16]	<b>0.34 <math>\pm</math> 0.13 [0.10 – 0.59]</b>
Female Age (Relative to 1 Year Old) <i>2+ Years Old</i>		-0.02 $\pm$ 0.14 [-0.28 – 0.24]	-0.08 $\pm$ 0.21 [-0.50 – 0.33]
Number of Helpers (Relative to 0) <i>1+ Helpers</i>		0.26 $\pm$ 0.13 [-0.01 – 0.51]	-0.07 $\pm$ 0.20 [-0.46 – 0.32]
Random Effects	$\sqrt{\text{Variance}} \pm \text{SD}$ [95% CI]	$\sqrt{\text{Variance}} \pm \text{SD}$ [95% CI]	$\sqrt{\text{Variance}} \pm \text{SD}$ [95% CI]
Cell ID	0.35 $\pm$ 0.19 [0.03 – 0.71] ( <i>n</i> = 741)	0.19 $\pm$ 0.13 [0.01 – 0.49] ( <i>n</i> = 448)	0.90 $\pm$ 0.18 [0.54 – 1.27] ( <i>n</i> = 301)
Female ID		0.52 $\pm$ 0.11 [0.28 – 0.74] ( <i>n</i> = 317)	0.81 $\pm$ 0.22 [0.33 – 1.24] ( <i>n</i> = 250)
Year	0.19 $\pm$ 0.08 [0.06 – 0.37] ( <i>n</i> = 11)	0.13 $\pm$ 0.10 [0.01 – 0.36] ( <i>n</i> = 11)	0.37 $\pm$ 0.17 [0.08 – 0.75] ( <i>n</i> = 11)
Spatial Correlation	2.21 $\pm$ 0.23 [1.71 – 2.62]	0.17 $\pm$ 0.09 [0.01 – 0.39]	0.14 $\pm$ 0.11 [0.00 – 0.41]
Zero Inflation Parameter	<i>n</i> = 8151 cell-years	<i>n</i> = 1138 female-nest-cell-years	<i>n</i> = 556 female-nest-cell-years